Nr4a1 Is Required for Fasting-Induced Down-Regulation of *Pparγ2* in White Adipose Tissue

Kalina Duszka, Juliane G. Bogner-Strauss, Hubert Hackl, Dietmar Rieder, Claudia Neuhold, Andreas Prokesch, Zlatko Trajanoski, and Anne-M. Krogsdam

Division of Bioinformatics (K.D., H.H., D.R., Z.T., A.-M.K.), Biocenter, Innsbruck Medical University, 6020 Innsbruck, Austria; and Institute for Genomics and Bioinformatics (J.G.B.-S., C.N., A.P.), Graz University of Technology, 8010 Graz, Austria

Expression of the nuclear receptor gene, *Nur77* (*Nr4a1*), is induced in white adipose tissue (WAT) in response to β-adrenergic stimulation and fasting. Recently, *Nur77* has been shown to play a gene regulatory role in the fasting response of several other major metabolic tissues. Here we investigated the effects of *Nur77* on the WAT transcriptome after fasting. For this purpose, we performed gene expression profiling of WAT from wild-type and *Nur77*$^{-/-}$ mice submitted to prolonged fasting. Results revealed *Nur77*-dependent changes in expression profiles of 135 transcripts, many involved in insulin signaling, lipid and fatty acid metabolism, and glucose metabolism. Network analysis identified the deregulated genes *Pparγ2* and *Nur77* as central hubs and closely connected in the network, indicating overlapping biological function. We further assayed the expression level of *Pparγ2* in a bigger cohort of fasted mice and found a significant *Nur77*-dependent down-regulation of *Pparγ2* in the wild-type mice ($P = 0.021$, n = 10). Consistently, the expression of several known *Pparγ2* targets, found among the *Nur77*-regulated genes (*i.e. G0s2*, *Grp81*, *Fabp4*, and *Adipoq*), were up-regulated in WAT of fasted *Nur77*$^{-/-}$ mice. Finally, we show with chromatin immunoprecipitation and luciferase assays that the *Pparγ2* promoter is a direct target of Nurr-related 77-kDa protein (Nur77)-dependent repressive regulation and that the N-terminal domain of Nur77 is required for this regulation. In conclusion, we present data implicating Nur77 as a mediator of fasting-induced *Pparγ2* regulation in WAT. **(*Molecular Endocrinology* 27: 135–149, 2013)**

Obesity and the obesity-related disorders, insulin resistance, hyperlipidemia, and hypertension, collectively known as the metabolic syndrome, are characterized as multifactorial in origin at several levels including underlying genetic variation. Combination drug treatment and personalized medicine are therefore emerging as the best option for increased control in this group of diseases. Activators of the nuclear receptor (NR) peroxisome proliferator-activated receptor γ (Pparγ) have already proven valuable in this context (1, 2) and are, along with peptide drugs and various insulin analogs, included in the panel of drugs currently applied in the clinic (3). However, the search for novel ways of further modifying the response to presently applied treatments is ongoing.

The Ppar subfamily of NRs is generally involved in metabolic regulation, particularly fat metabolism (4). It comprises three members: Pparα (Nr1c1), Pparβ/δ (Nr1c2, FAAR), and Pparγ (Nr1c3). Due to alternative promoter use at the *Pparγ* gene, several isoforms of Pparγ exist (5, 6), with the Pparγ2 isoform being of particular interest in terms of insulin sensitization and pro-lipogenesis (4, 7–9). Pparγ2 plays a pivotal role in adipogenesis and in the function of mature adipocytes (4, 10). By reg-

ISSN Print 0888-8809 ISSN Online 1944-9917
Printed in U.S.A.

doi: 10.1210/me.2012-1248 Received July 30, 2012. Accepted October 29, 2012.
First Published Online December 18, 2012

Abbreviations: BAT, Brown adipose tissue; ChIP, chromatin immunoprecipitation; ChIP-seq, ChiP sequencing; DAPI, 4′,6-diamidino-2-phenylindole; EST, expressed sequence tag; GERP, Genomic Evolutionary Rate Profiling; HFD, high-fat diet; IPA, Ingenuity Systems Pathway Analysis; NBRE, Nur77 binding response element; NR, nuclear receptor; Nur77, Nurr-related 77-kDa protein; Pparγ, peroxisome proliferator-activated receptor γ; PPRE, Ppar response element; qPCR, quantitative real-time PCR; SDS, sodium dodecyl sulfate; TSS, transcription start site; WAT, white adipose tissue.

ulating a host of target genes, it influences glucose metabolism, lipid transport, fatty acid uptake, and recycling of intracellular fatty acid, promoting lipid storage and lipogenesis. In healthy adipose tissue, Pparγ guarantees a metabolically balanced and adjusted regulation of secretion of adipocytokines such as adiponectin and leptin, which are major contributors to a regular insulin response (11–13). Pparγ activators are mainly found in the form of ligands that bind Pparγ and enhance the transcriptional activator function of Pparγ heterodimerized with the retinoid X receptor (Rxr, Nr2b family), bound to Ppar response elements (PPREs) in promoters of Ppar-responsive target genes (4, 14–17). An ongoing search for further factors involved in the regulatory function of Pparγ has recently brought several previously less characterized genes to attention (18, 19).

Recent studies have highlighted a possible metabolic regulatory role of a different NR subfamily, the NR4as.

Members of the Nr4a family include Nurr-related 77-kDa protein (Nur77, Nr4a1, Ngf-Ib, and Tr3), Nurr1 (Nr4a2), and Nor-1 (Nr4a3). They are expressed as early-response genes in response to a number of physiological and pathophysiological stimuli, such as adrenergic hormones, glucose, insulin, fatty acids, growth factors, cytokines, and the pro-anorexic melanocortin α-MSH (20, 21). The Nr4as are implicated in various biological processes, including carcinogenesis/apoptosis control, inflammation, vascular disease, and metabolism (22–24).

Nur77 has the most widespread tissue distribution of the Nr4a members. Notably, it is known to be expressed in metabolically demanding and energy-dependent tissues (25). Recently, several research groups have shown that β-adrenergic signaling stimulates *Nur77* expression in major metabolic tissues under distinct physiological conditions (26–30). It affects glucose homeostasis and oxidative metabolism in skeletal muscle, gluconeogenesis, and lipogenesis in liver, glycogen utilization in heart, and energy expenditure in brown adipose tissue (BAT) and possibly white adipose tissue (WAT) (21, 27, 29–38). Nur77 has been proposed as a direct regulator of several genes in liver, muscle, BAT, and WAT, but only a small number of direct target genes have been verified. Nur77 regulates transcription of its target genes through binding to promoter response elements. As a monomer, it binds Nur77 binding response elements (NBREs). As a homodimer, or heterodimerized with Nurr1 (Nr4a2) or with Rxr, it binds NURR-responsive elements (23, 24). No natural, physiological ligand has been identified for the Nr4as, but several activators have been described (39–42), including a molecule with true ligand qualities, cytosporone B, isolated from a tropic, endophytic fungus (43).

The emerging role of *Nur77* as an early-response gene in metabolic regulation primarily indicates a strong metabolic transition-modifying role, particularly with emphasis on a positive role in glucose homeostasis and a distinct anti-lipogenic role. In several studies, *Nur77* expression has been demonstrated capable of blocking adipogenesis in cell-culture models (44–46).

Although several investigations have identified a metabolic regulatory role of *Nur77* in WAT,the underlying mechanisms have remained elusive. When kept on a standard chow diet, the *Nur77*$^{-/-}$ mouse displays no apparent phenotype (47). When raised on a high-fat diet (HFD), it exhibits increased weight gain and insulin resistance (32). In the present study, we addressed this issue, applying transcriptome analysis of epididymal WAT from fasted *Nur77*$^{-/-}$ mice and their wild-type littermates. Mapping the differentially expressed genes against a bibliography-based network database revealed a high-scoring network with *Nur77* and *Pparγ* as neighboring major hubs. *Pparγ2* has been reported to be down-regulated in WAT depots from fasted mice (48). In *Nur77*$^{-/-}$ mice, we found this down-regulation significantly impaired. We further show that the blunted down-regulation of *Pparγ2* is reflected in increased expression of the known downstream mediators of Pparγ2 function, *Lep*, *Fabp4*, *Adipoq*, *Grp81*, and *G0s2*. Finally, we show that Nur77 directly binds and represses the *Pparγ2* promoter, implicating that the metabolic homeostatic functions of *Nur77* partly results from modified *Pparγ2* expression.

Materials and Methods

Plasmids

The viral expression vectors pBabe-Nur77, pBabe-Nur77DN, and pBabe were kindly provided by Wen Chen Yeh (49). *Pparγ2* promoter fragments [−2327/+62, −1078/+62, and −1078/−768 bp relative to the transcription start site (TSS)] were cloned from Black6 mouse genomic DNA using the primers *PmPPg2* −2327 (*Sac*I) forward, 5′-catt**gagctc**atcccttggaagaaggttgg; *PmPPg2* −1078 (*Sac*I) forward, 5′-catt**gagctc**a cactgccctgtgtaagggctc; *PmPPg2* +62(*Bam*HI) reverse, 5′-gatctt**ggat**ccggcagtgcatcagcgaaggc; and *PmPPg2* −768(*Bgl*II) reverse, 5′-catt**agatct**actgcagtagtattccaatgg (cloning sites in bold). The fragments were verified by sequencing and cloned into the luciferase reporter vectors: pGl4.26 (containing a minimal promoter) and pGl4.21 (without a minimal promoter) (both from Promega, Mannheim, Germany). *Bgl*II, *Sac*I and *Bam*HI restriction sites of the vectors were used. The inducible Tet-off-Nur77 expression vector was generated by cloning mouse Nur77 into pTRE-Tight (Clontech-Europe, Vienna, Austria) downstream from the Tet-responsive Ptight promoter, using *Eco*RI and *Bam*HI restriction sites. Successful cloning was confirmed by sequencing.

Cell culture

3T3-L1 fibroblasts were maintained in high glucose (4.5 g/liter) DMEM supplemented with 10% fetal bovine serum, 33.7 μM pantothenic acid, 32 μM biotin, 2 mM L-glutamine, 100 U/ml penicillin, 100 U/ml streptomycin (all from Life Technologies, Vienna, Austria) and Normocin (Invivogen/Eubio, Vienna, Austria) under a humidified atmosphere of 5% CO_2 at 37 C. Two days past confluence, adipogenesis was induced with medium containing a standard cocktail (1 μM dexamethasone, 500 μM 3-isobutyl-1-methylxanthine, and 1 μg/ml insulin; all from Sigma-Aldrich, Vienna, Austria) along with 1 μM rosiglitazone (Eubio, Vienna, Austria). Medium was changed every 2 d, leaving out dexamethasone and 3-isobutyl-1-methylxanthine after the first 2 d and insulin and rosiglitazone after 4 d. Approximately 98% of the cells became fully differentiated (Supplemental Fig. 1, published on The Endocrine Society's Journals Online web site at http://mend.endojournals. org). For the isoprenaline induction studies, the day before medium was changed to low-glucose (1 g/liter), phenol red-free DMEM (Life Technologies) with 3% BSA (Sigma-Aldrich). After overnight incubation, at 0 h, 1 μM isoprenaline (Sigma-Aldrich) was added to the medium. Samples were harvested at 0, 2, 4, 6, 8, and 12 h in Trizol (Life Technologies). NIH 3T3-L1 cell were maintained in high-glucose (4.5 g/liter) DMEM supplemented with 10% FBS (Sigma-Aldrich), 2 mM L-glutamine, 100 U/ml penicillin, and 100 U/ml streptomycin (all from Life Technologies) and Normocin (Invivogen/Eubio) at 5% CO_2 and 37 C. Nur77 silencing in 3T3-L1 cells was achieved by transduction of preconfluent 3T3-L1 cells with retroviral constructs expressing a short hairpin sequence targeting Nur77 or a control sequence (nontargeting). The viral preparations were obtained from Sigma-Aldrich. The transduced cells were selected under puromycin (Sigma-Aldrich) and maintained as polyclonal cultures and differentiated into mature adipocytes (as described above).

Animal experiments

Nur77$^{-/-}$ C57BL/6 mice were kindly provided by Prof. M. Klingenspor (Munich Technical University, Munich, Germany). All mice were kept on a 12-h light, 12-h dark cycle and housed according to institutional guidelines and approved by the Austrian Bundesministerium für Wissenschaft und Forschung. Unless otherwise indicated, the mice were kept on a standard laboratory chow diet with free access to water. For fasting experiments, the mice were fasted 20–24 h, with free access to water, before being killed by cervical dislocation followed by dissection of epididymal fat pads. For refeeding experiments after overnight fasting, the mice were given free access to food for 2 or 8 h before being killed. Where indicated, the mice were given a HFD (D12331; Research Diets, Inc., New Brunswick, NJ) for 6 wk during which time they were housed in separate cages before fasting and being killed.

RNA isolation

RNA isolation from cells and tissues was done with Trizol according to the manufacturer's recommendations (Life Technologies). RNA concentrations were determined with a NanoDrop spectrophotometer (Thermo Scientific, Vienna, Austria). The quality of the RNA was verified with the 2100 bioanalyzer from Agilent (Agilent Technologies, Vienna, Austria).

Quantitative real-time PCR (qPCR) analysis

Superscript II and random primers were used for the reverse transcription step. The qPCR reactions were performed with the ABI Prism 7000 (Life Technologies), using SYBR green Platinum Mastermix (Life Technologies). Each reaction was done in three technical replicates. Primer sequences are listed in Supplemental Table 2. Raw data were analyzed using the Analyzer-Miner algorithms (50) inherent in the software RT-PCR database (https://rtpcr.genome.tugraz.at/rtpcr/) (51). All values were normalized against *Uxt*. Statistical tests were done with two-sided Student's *t* test. Error bars on diagrams represent SE. Primer sequences are listed in Supplemental Table 3.

Microarrays

Total RNA was reverse transcribed with SuperScript II and random hexamer primers (Life Technologies) under incorporation of amino-allyl-dUTP allowing for subsequent indirect labeling with Cy3/Cy5 dyes. Four individual *Nur77*$^{-/-}$ mouse RNA samples were hybridized, against pooled RNA from the *Nur77*$^{+/+}$ siblings, to cDNA microarrays. The cDNA microarrays applied were developed in-house with a focus on expressed sequence tags (ESTs) expressed in adipose tissues (52). Dye swaps were performed. The resulting relative dye intensities were obtained through scanning at 10-μm resolution in an Axon GenePix 4000B scanner (Biozym, Vienna, Austria). Low-intensity, inhomogeneous, and saturated spots were filtered out using GenePix Pro version 4.1 (Biozym). The results were normalized and statistically evaluated in CARMAWeb (53) using within-slide median normalization with background subtraction and scale normalization between slides. Values were averaged between replicates. To alleviate the loss of power from the formidable multiplicity of gene-by-gene hypothesis testing that is common to microarray experiments, a nonspecific prefiltering was carried out using the 40% of the genes with the biggest variance over the samples, leaving 11,659 expression profiles for further analysis. Differential expression was evaluated with the moderated *t* test from the Limma package (54). Additionally, the method proposed by Hochberg and Benjamini (55) (false discovery rate <0.05) was applied. The resulting list of expression profiles was further filtered to exclude profiles with less than 1.5-fold differential expression. Among the 186 differentially expressed ESTs, 146 could be assigned to RefSeq IDs. Of those, 11 were temporary RefSeq IDs and thus excluded, leaving 135 RefSeq Gene IDs to be included in further analysis. The microarray data are available at ArrayExpress: E-MEXP-3771.

Bioinformatic analysis of differentially expressed genes

Functional and bibliography-based network analysis was performed with the Genomatix (www.genomatix.de) and Ingenuity Systems Pathways Analysis (IPA) Core Analysis (www.ingenuity.com) as indicated. Because the *Nr4a1* EST on the microarray chips was compromised, the *Nr4a1* ID was manually added to the list, for the sake of relevance. Particularly, for the IPA Core Analysis, first, a stringent setting, matching only networks annotated for adipose tissue, was selected, rendering only 58% of the uploaded genes eligible for network mapping. The resulting network score brought out "lipid metabolism" with a score of 46, and *Nr4a1*, *Pparγ*, *Ctnnb1*, and *IL4* as central hubs.

However, a less stringent analysis allowing inclusion of molecules and networks not previously described in adipose tissues (by selecting "all tissues and cell lines") rendered 82% of the uploaded genes eligible for mapping and brought out the network finally applied (see Fig. 2). The selection of relevant subnetworks in the IPA algorithm is based in part on the assumption that biological function correlates with locally dense molecular interactions. Networks are generated by first identifying focus genes (genes having many specific connections within the submitted gene list relative to their total, global, number of gene connections). Based on connectivity, the network is then allowed to extend from these focus genes. The p-score is the $-\log10$ representation of the P value (the probability of finding f or more focus genes in a set of n genes randomly selected from the global molecular network), calculated using Fisher's exact test (56). The 135 RefSeq assigned genes were further investigated with respect to Pparγ binding sites by comparison with published chromatin immunoprecipitation sequencing (ChIP-seq) data from mature adipocytes (data kindly provided by Refs. 57 and 58) and scanned for putative NBREs with the MatInspector tool from Genomatix using a core similarity of at least 75% and optimized matrix similarity. Gene2Promoter was used to obtain sequences from 2000 bp upstream from the first RefSeq TSS to 500 bp downstream of the last RefSeq TSS.

Western blot

Tissue protein extracts were generated by homogenizing epididymal mouse fat pads under liquid N_2, dissolving in RIPA buffer, and sonicating using a Bioruptor sonicator. Sonicated samples were dissolved 1:1 in standard Laemmli sample buffer (without blue dye), incubated at 96 C for 5 min, and cleared at $20000 \times g$ for 15 min. Cell culture protein extracts were prepared by direct lysis in Laemmli sample buffer (without blue dye) and similarly cleared. Protein quantification was done with the Pierce BCA Protein Assay Kit (Fisher scientific, Vienna, Austria). The protein was separated on 12% Bis-Tris NuPAGE Novex gels (Life Technologies), and 50 μg 3T3-L1 protein extract or 25 μg mouse extract was loaded per lane. Blotting was onto nitrocellulose membranes. The Nur77, FABP4 (fatty acid-binding protein 4), and β-actin antibodies were from Santa Cruz Biotechnology (Santa Cruz, CA), the PPARγ antibody was from Cell Signaling (NEB, Vienna, Austria). Secondary horseradish peroxidase-conjugated antibodies were from Dako Osterreich (Vienna, Austria). Imaging was done applying ECL West Dura substrate (Pierce) and imaging on a MicroChemie imaging station (DNR Bio-Imaging Systems, Vienna, Austria).

Immunofluorescence

Cells were grown and differentiated (as above) on coverslips and fixed using 3.5% paraformaldehyde in PBS. Nur77 was detected by a rabbit anti-Nur77 antibody and visualized with a secondary chicken antirabbit antibody coupled to Alexa Fluor-488. Nuclei were counterstained with 4′,6-diamidino-2-phenylindole (DAPI). Images were collected on a Zeiss AxioImager Z1 equipped with an AxioCam Mrm CCD camera using a ×40 0.75 numerical aperture and ×63 1.4 numerical aperture lens. All images in all conditions were recorded by the same microscope parameter settings at the same exposure times.

Promoter analysis and ChIP-qPCR

The mouse *Pparg2* promoter sequence was extracted from the CSHL promoter database (http://rulai.cshl.edu/CSHLmpd2/). Conservation analysis [Genomic Evolutionary Rate Profiling (GERP) score] of the mouse *Pparg2* promoter sequence was done using ENSEMBL (www.ensembl.org). A promoter scan was performed using MatInspector from Genomatix (www.genomatix.de) with the NBRE position weight matrix. The analysis revealed five putative Nur77 binding sites. ChIP with qPCR readout (ChIP-qPCR) was carried out on nuclear extract from 3T3-L1 cells, stably expressing Nur77 (3T3-L1/pBabe-Nur77), with an antibody against Nur77 (M210; Santa Cruz). Cells were cross-linked with 1% formaldehyde for 20 min. Nuclei were isolated in hypotonic lysis buffer [20 mM HEPES (pH 8.0), 10 mM EDTA, 0.5 mM EGTA, 0.25% Triton X-100]. Nuclear chromatin was extracted in nuclear lysis buffer [50 mM HEPES (pH 8), 1 mM EDTA, 0.5 mM EGTA, 0.1% sodium dodecyl sulfate (SDS)] and sonicated five times for 20 sec each at 40% output with a Bandelin sonicator. Ten microliters were saved as input. ChIP was done with 60–80 μg chromatin diluted to 0.8–1 μg/μl in immunoprecipitation buffer [final concentration, 20 mM HEPES (pH 8), 2 mM EDTA, 1 mM EGTA, 1% Triton X-100, 0.15 M NaCl, 0.07% SDS, 1 mg/ml BSA] with the Nur77 antibody or with nonimmune IgG (Santa Cruz). After overnight incubation with antibody and A/G Plus agarose beads (Santa Cruz), preblocked with 1 mg/ml BSA, the beads were isolated and washed once in WB1 [20 mM HEPES (pH 8), 150 mM NaCl, 1 mM EDTA, 0.5 mM EGTA, 0.1% SDS, 1% Triton X-100, 0.1% Na-deoxycholate], once in WB1 high salt (WB1 with 500 mM NaCl), once in WB2 [20 mM HEPES (pH 8), 0.25 M LiCl, 1 mM EDTA, 0.5 mM EGTA, 0.5% IGEPAL CA-630 (octylphenoxypolyethoxyethanol), 0.5% Na-deoxycholate), and twice in HEE buffer [20 mM HEPES (pH 8), 1 mM EDTA, 0.5 mM EGTA]. Immunoprecipitated chromatin (on the beads) and the input samples were reverse cross-linked, extracted, and purified with phenol/$CHCl_3$ extraction and ethanol/Na-acetate precipitation. All buffers except the HEE buffer were supplemented with protease inhibitor cocktail (Roche Diagnostics GmbH, Mannheim, Germany) and phenylmethylsulfonyl fluoride. Fold enrichment was determined with qPCR (as described above). The amount of DNA in the qPCR was calculated relative to the input DNA by comparison of the S18 amplicon quantification cycles to a standard curve generated from the input DNA. Final enrichment was calculated against the IgG samples (to eliminate general IgG effects), relative to a non-NBRE site of the *Pai-1* promoter (to count out any general background effects of the Nur77 antibody). Detectors for a known NBRE in the *Pai-1* promoter served as a positive control (59).

Luciferase reporter assays

NIH-3T3 cells were seeded at 10,000 cells per well in 96-well plates. The next day, transfection was carried out using MetafectenePro (Biontex, Martinsried, Germany) in ratio of 3:1 (microliters MetaFectenePro to micrograms DNA) following the provider's instructions. One hundred nanograms of luciferase reporter vectors of pMSCV-*Cebpα* as well as a titration of pBABE-*Nur77* and pBABENur77DN (10, 50, 75, and 100 ng) was used. Addition of empty pMSCV and pBABE vectors was calculated to balance the promoter load.

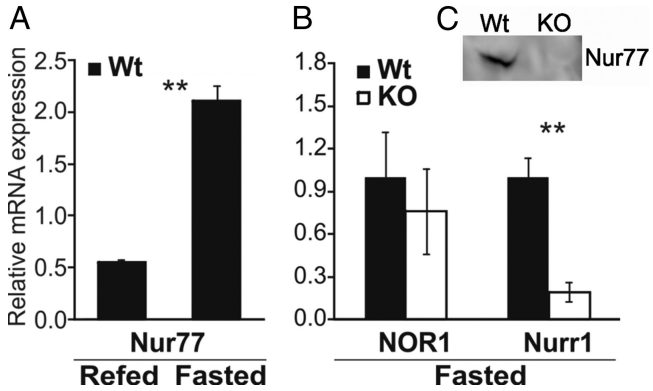

FIG. 1. Expression of Nr4as in WAT from fasted mice. A, qPCR-based *Nur77* expression analysis of WAT mRNA from wild-type (Wt) mice, either fasted or overnight fasted followed by 8 h refeeding (n = 3). *, $P < 0.05$. B, qPCR-based analysis of *NOR1* and *Nurr1* expression in WAT mRNA from fasted wild-type and *Nur77*$^{-/-}$ mice (n = 6). *, $P <$ 0.05. C, Western blot showing expression of *Nur77* in fasted wild-type (Wt) but not *Nur77*-knockout (KO) mice WAT.

pBluescript was used as fill DNA. As a control for varying transfection efficiencies, Renilla reporter vector pGl4.75 (Promega) was cotransfected in all the experiments in a ratio of 1:100 to luciferase reporter vectors. After 48 h, the cells were lysed and assayed following the dual-luciferase assay system (Promega) protocol. Luminescence measurements were obtained with an Orion II luminometer (Berthold Technologies, Vienna, Austria). "Relative light units" denotes the ratio of luciferase to renilla values. A two-sided Student's *t* test was applied for statistical evaluation. Error bars on the diagrams represent SD.

Results

Nur77-dependent gene expression in fasting WAT

Expression of members of the *Nr4a* family is induced in WAT during fasting (26–29, 32, 60). To investigate functional role of the *Nur77* induction, we subjected *Nur77*$^{-/-}$ mice and their wild-type siblings to prolonged fasting with or without subsequent refeeding for 8 h (Fig. 1). *Nur77* expression in WAT was induced under fasted compared with refeeding conditions (Fig. 1A). In the absence of *Nur77*,the other family members (*Nurr1* and *Nor1*) known to be capable of exhibiting *Nur77* overlapping functions were not further induced at the transcriptional level (Fig. 1B). In fact, *Nurr1* expression was significantly down-regulated in the absence of *Nur77* expression. Previous reports have shown that silencing of one family member can lead to increased expression of the others, partly substituting the function of the silenced member (26). Because no compensatory expression increase was observed for *Nurr1* or *Nor1*, we performed expression profiling of the adipose tissue from fasted *Nur77*$^{-/-}$ and wild-type mice. To confirm that the *Nur77*$^{-/-}$ genotype remained conserved at the protein expression level, we performed Western blotting of total protein obtained from fasted wild-type and *Nur77*$^{-/-}$ mouse fat pads (Fig. 1C).

To directly measure differential expression related to the *Nur77*$^{-/-}$ genotype, total RNA isolated from the epididymal fat pads of every individual fasted *Nur77*$^{-/-}$ mouse were hybridized on cDNA microarrays (43) against a pool of RNA from fasted wild-type mice. From 186 significantly differentially expressed ESTs between the *Nur77*$^{-/-}$ and wild-type mice ($P <$ 0.1, >1.5-fold change), 135 could be annotated by RefSeq, and were considered for further analysis (Supplemental Table 1).

Top genes with higher expression in the *Nur77*$^{-/-}$ mice included the protein phosphatase 2, catalytic subunit A, (*Pp2a*)-interacting centromere guardian Shugoshin-like 1 (*Sgol1*) (61), the E3 ubiquitin ligase regulating the amplitude of protein kinase C signaling, tripartite motif containing 41 (*Trim41*) (*RINCK* ortholog) (62), and the adipokine leptin (*Lep*). Genes with highly reduced expression in the *Nur77*$^{-/-}$ mice included the transcriptional cosupressor, brain abundant, membrane attached signal protein 1 (*Basp1*) (63), the WNT signaling regulator, β-catenin (*Ctnnb1*) (80-kDa variant) (64), and the G protein-coupled receptor signal regulator, receptor (calcitonin) activity modifying protein 3 (*Ramp3*) (65). A large proportion of the 135 differentially expressed genes encode proteins with transcriptional regulatory or signal-modifying function. Because even a small relative change in abundance of these proteins can affect large functional amplitude, the full list of genes (Supplemental Table 1) was included in further analysis.

Applying gene ontology classification (Genomatix GePS tools) analysis revealed that metabolic processes within the categories cellular process ($P = 4.95 \times 10^{-10}$), regulation of biological quality ($P = 6.06 \times 10^{-7}$), and cellular catabolic process ($P = 1.45 \times 10^{-6}$) were most significantly overrepresented (Supplemental Table 2). Extending the predicted functional classification to biological pathway analysis, we found significant enrichment for the hepatocyte growth factor pathway ($P = 3.35 \times 10^{-5}$) and for the Pparγ signaling pathway ($P = 4.06 \times 10^{-4}$) (Table 1). Curated, bibliography-based association analysis (IPA Core Analysis, Ingenuity) for the identification of molecular and cellular functions revealed two highly significant themes: drug metabolism (P range = 4.66×10^{-7} to 7.73×10^{-3}) and lipid metabolism (P range = 1.20×10^{-7} to 7.73×10^{-7}) (Table 2).

We further performed network analyses of differentially expressed genes based on connectivity information retained in a knowledge base (IPA, Ingenuity). The network "drug metabolism, glutathione depletion in liver,

TABLE 1. Top pathway associations (GePS pathway analysis) for genes differentially expressed in WAT of fasted *Nur77*$^{-/-}$ mice

Pathway ID	Pathway	*P* value	List of observed genes
PW_HGF	Hepatocyte growth factor receptor	3.35×10^5	*Adm*, *Med1*, *Ctnnb1*, *Krt18*, *Spint2*, *Rps6ka1*, *Csf1*, *Mat2a*, *Sat1*, *Pparg*, *Mtap2*, *Hmox1*, *Mmp7*
PW_PPARG	Pparγ	4.06×10^4	*Med1*, *Ctnnb1*, *Fabp4*, *Nr4a1*, *Rps6ka1*, *Sat1*, *Pparg*, *Hmox1*, *Nucb2*, *Ptgds*, *Lep*, *Npy*
PW_LEPTIN	Leptin receptor	1.04×10^3	*Pdia3*, *Mt2*, *Ctnnb1*, *Fabp4*, *Rps6ka1*, *Mat2a*, *Pparg*, *Nucb2*, *Lep*, *Npy*
PW_PLA2	Phospholipase A2	1.52×10^3	*Pdia3*, *Apod*, *Ctnnb1*, *Acsl4*, *Rps6ka1*, *Csf1*, *Pparg*, *Ptgds*, *Lep*
PW_CALCINEURIN	Calcineurin (protein phosphatase 3)	1.88×10^3	*Pdia3*, *Ctnnb1*, *Kcnip3*, *Nr4a1*, *Pparg*, *Mtap2*, *Hmox1*, *Hdc*, *Ptgds*, *Lep*, *Npy*
PW_CASPASE	Caspase	5.00×10^3	*Pdia3*, *Il16*, *Mpz*, *Ctnnb1*, *Kcnip3*, *Krt18*, *Krt8*, *Nr4a1*, *Rps6ka1*, *Csf1*, *Sat1*, *Pparg*, *Mtap2*, *Hmox1*, *Dffa*, *Ptgds*, *Lep*
PW_CAMK	Calcium/calmodulin-dependent protein kinase	6.12×10^3	*Pdia3*, *Apod*, *Ctnnb1*, *Kcnip3*, *Nr4a1*, *Rps6ka1*, *Pparg*, *Mtap2*, *Hmox1*, *Npy*
PW_ADCY	Adenylate cyclase	6.63×10^3	*Adm*, *Ctnnb1*, *Nr4a1*, *Rps6ka1*, *Hdc*, *Ptgds*, *Lep*, *Npy*
PW_EGF	Epidermal growth factor receptor family member ErbB4	6.78×10^3	*Pdia3*, *Clca1*, *Stard10*, *Acly*, *Mpz*, *Med1*, *Ctnnb1*, *Fabp4*, *Gstm1*, *Krt8*, *Nr4a1*, *Rps6ka1*, *Csf1*, *Epcam*, *Pparg*, *Mtap2*, *Hmox1*, *Hdac6*, *Hdc*, *Mmp7*, *Lep*, *Npy*
PW_14 3 3	14 3 3 protein	7.34×10^3	*Ctnnb1*, *Krt18*, *Krt8*, *Rap1gap2*, *Nr4a1*, *Rps6ka1*
PW_ADRENORECEPTOR	Adrenergic receptor	7.46×10^3	*Nr4a1*, *Pparg*, *Mtap2*, *Mmp7*, *Lep*
PW_CDKN1	Cyclin dependent kinase inhibitor 1	7.56×10^3	*Ctnnb1*, *Nr4a1*, *Rps6ka1*, *Csf1*, *Ly6e*, *Sat1*, *Pparg*, *Hmox1*, *Lep*
PW_PKC	Protein kinase C	8.52×10^3	*Pdia3*, *Adm*, *Crabp2*, *Acly*, *Mpz*, *Med1*, *Ctnnb1*, *Fabp4*, *Ehf*, *Marcksl1*, *Krt18*, *Krt8*, *Mt1*, *Nr4a1*, *Pebp1*, *Rps6ka1*, *Csf1*, *Ly6e*, *Soat1*, *Trim41*, *Ramp3*, *Pparg*, *Mtap2*, *Hmox1*, *Hdc*, *Ptgds*, *Lep*, *Npy*
PW_RXR	Retinoid X receptor	9.29×10^3	*Crabp2*, *Med1*, *Ctnnb1*, *Nr4a1*, *Pparg*

The 148 differentially expressed (false discovery rate = 10) genes, extracted from the microarray expression analysis of RNA from fasted WAT from *Nur77*$^{-/-}$ mice hybridized against RNA from fasted WAT from their wild-type siblings (n = 4), were submitted to Genomatix GePS pathway analysis. Pathways with significant hits ($P < 0.01$) are listed [*P* values (*t* test) represent the probability that the network hit was random].

lipid metabolism" appeared as the highest scoring network, covering 46% of the differentially expressed genes and representing 50% of the network molecules (Table 3). The genes associated with this network are marked in the total gene list in Supplemental Table 1. Visualization of the expression data, mapped on this network, highlighted three major hubs [*Pparγ*, *Nur77* (*Nr4a1*), and *Ctnnb1*] with a direct connection between *Pparγ* and *Nr4a1* (Supplemental Fig. 2). The selection of relevant subnetworks in the IPA algorithm is based in part on the assumption that biological function correlates with locally dense molecular interactions. The algorithm further

TABLE 2. Top biological functions: molecular and cellular functions (IPA Core Analysis)

Name	*P* value	Molecules
Drug metabolism	4.66×10^7 to 7.73×10^3	9
Lipid metabolism	1.20×10^6 to 7.73×10^3	28
Small molecule biochemistry	1.20×10^6 to 7.73×10^3	34
Cellular compromise	1.52×10^5 to 7.73×10^3	13
Cellular assembly and organization	2.69×10^5 to 7.73×10^3	16

Ingenuity IPA Core Analysis was applied to detect the top biological functions (*P* values represent right-tailed Fisher's exact *t* test values covering the associated molecules)

TABLE 3. Top networks (IPA Core Analysis)

ID	Associated network functions	*P* score
1	Drug metabolism, glutathione depletion in liver, lipid metabolism	127
2	Cellular assembly and organization, nervous system development and function, organ morphology	75
3	Cellular growth and proliferation, renal and urological system development and function, cell-to-cell signaling and interaction	2
4	Cancer, genetic disorder, respiratory disease	2

Ingenuity IPA Core Analysis was applied to detect the top networks covered by the dataset, based on the bibliography-associated, curated Ingenuity network database. The *P* score is the −log10 representation of the *P* value (the probability of finding *f* or more focus genes in a set of *n* genes randomly selected from the Global Molecular Network), calculated using Fisher's exact test.

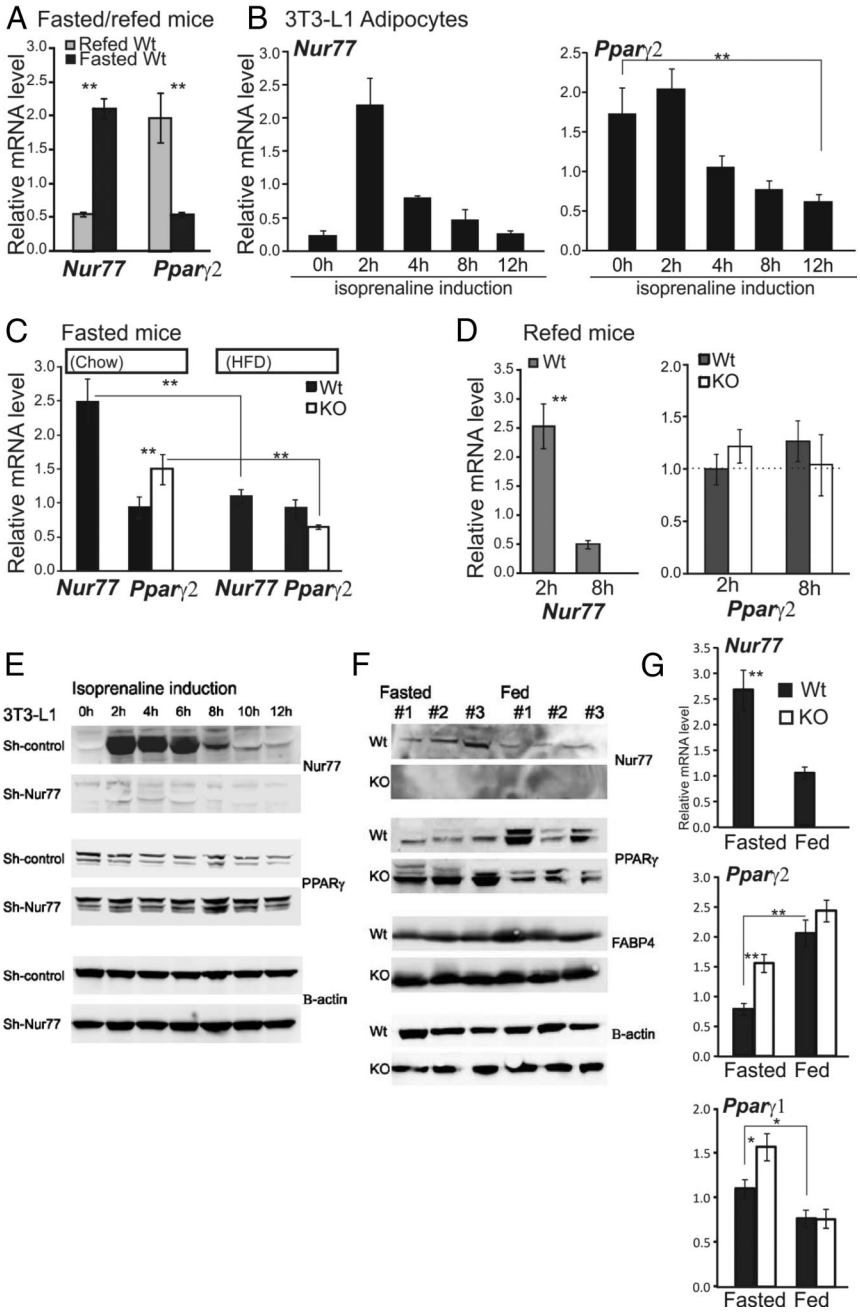

FIG. 2. Expression of *Nur77* and *Pparγ2* in white adipocytes. Expression (mRNA) levels (qPCR) of *Nur77* and *Pparγ2* were determined for the following: A, WAT harvested from wild-type (Wt) mice, either fasted or fasted followed by 8 h refeeding (n =3); B, Mature 3T3-L1 adipocytes were stimulated with isoprenaline (1 μM at 0 h); C, WAT of 24-h fasted *Nur77*$^{-/-}$ [knockout (KO)] mice and their Wt littermates kept on either regular chow (n = 7) or HFD (n = 5); D, *left panel*, WAT of Wt mice overnight fasted and refed for 2 and 8 h (n ≥ 4); *right panel*, WAT of Wt and *Nur77*$^{-/-}$ mice (KO) fasted overnight and refed for 2 and 8 h (n ≥ 3). The Wt 2-h refeeding was set to 1. *, $P < 0.05$; **, $P < 0.01$. E, Western blot showing protein analyses in protein extracts from 3T3-L1 adipocytes with (Sh-Nur77) or without (Sh-control) silencing of Nur77. Sh, Short hairpin silencing construct. Protein was harvested at the indicated time points after isoprenaline induction. β-Actin was included as loading control. The images shown are representative of three biological replicate experiments. F, Western blot showing protein analyses in protein extracts from WAT from fasted or fed Wt or *Nur77*$^{-/-}$ (KO) mice. Three mice are shown for each condition. G, Expression (mRNA) levels (qPCR) of *Nur77*, *Pparγ2*, and *Pparγ1* were determined for the cohort of mice used for Western blot (fasted mice, n ≥ 10; fed mice, n ≥ 3).

takes into account that some molecules (*e.g.* PPARγ) have more known interactions than the average molecule and attempts to counter such bias. The immediate proximity of *Pparγ* and *Nur77* (*Nr4a1*) implies predicted overlapping biological function.

In summary, these analyses suggest that Pparγ and Pparγ-dependent functions are central components of the *Nur77*-dependent, differential expression profile in fasted WAT.

Down-regulation of *Pparγ2* expression during fasting is *Nur77* dependent

To further investigate the relative expression of *Pparγ* and *Nur77* in WAT under various metabolic conditions, we performed qPCR analyses.

As shown in Fig. 2A, the *Nur77* expression was significantly induced in WAT of fasted mice, whereas the *Pparγ2* mRNA level was significantly decreased in WAT from fasted compared with refed (8 h refed) animals. Similar expression patterns were observed in a time-resolved manner, when mature 3T3-L1 adipocytes were serum starved in a low-glucose medium and stimulated with the β-adrenergic agonist isoprenaline (1 μM) (Fig. 2B). Briefly, the *Nur77* mRNA expression increased rapidly after isoprenaline treatment as expected based on previous reports (26, 27, 29, 66), whereas the *Pparγ2* expression level decreased during the 12 h of isoprenaline treatment.

In contrast, in the absence of *Nur77* (in WAT from fasted *Nur77*$^{-/-}$ mice), the *Pparγ2* expression was significantly less decreased (Fig. 3C, *left panel*). The gene expression profiles of *Pparγ2* and *Nur77* were further assayed in WAT of *Nur77*$^{-/-}$ and wild-type mice kept on a HFD before fasting. In the mice on HFD, the fasting-induced *Nur77* expression level was far less pronounced than in the chow mice (Fig. 3C, *right panel*). Concomitantly, the *Pparγ2* expression level was

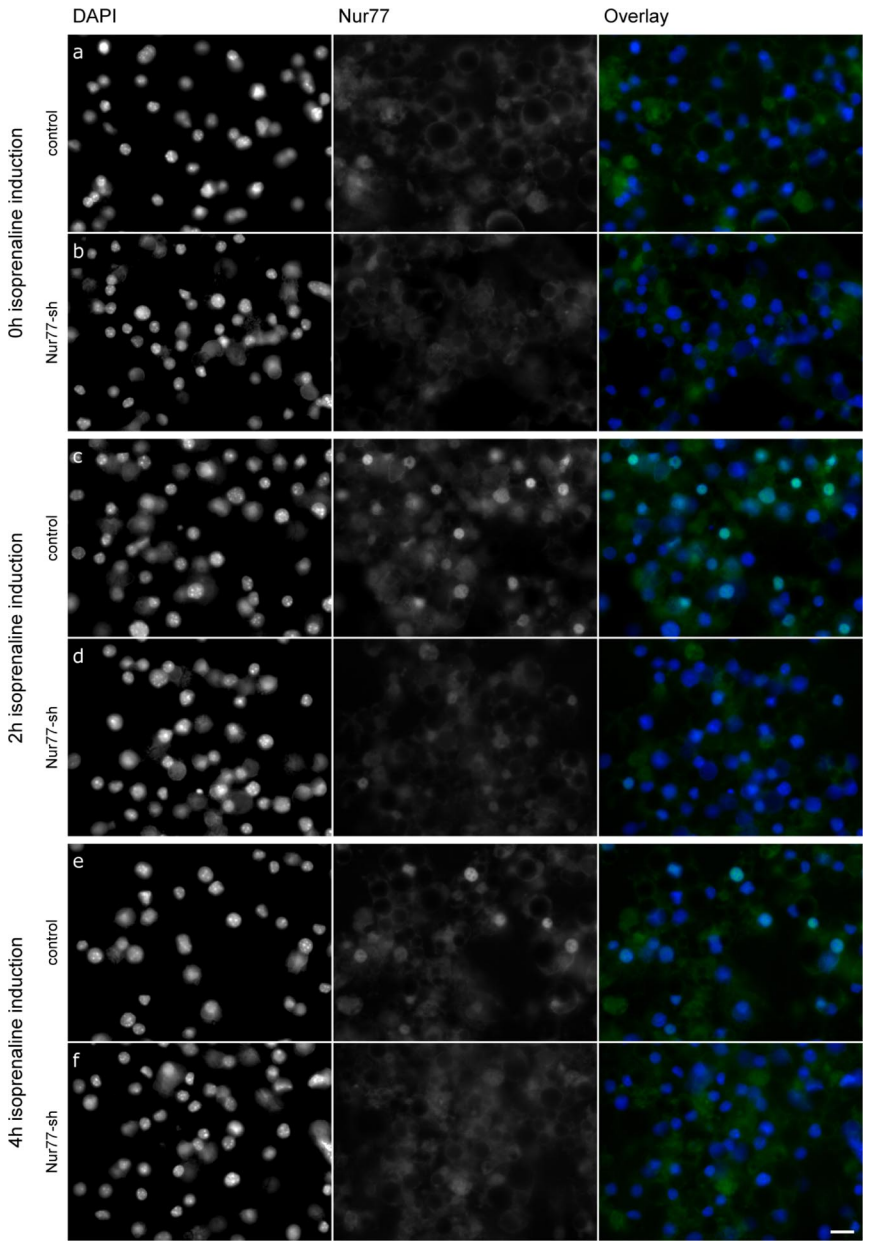

FIG. 3. Nuclear Nur77 localization imaging. Fluorescent images of mature adipocytes [with Nur77 silencing (Nur77-sh) or without (control)] stained with the nuclear stain DAPI and with anti-Nur77 antibody and visualized with Alexa dye-coupled secondary antibody at the indicated time points after isoprenaline induction.

not significantly altered in response to fasting in the HFD-subjected mice, indicating an altered *Pparγ2* expression regulation in the HFD mice.

In addition to being induced in response to fasting, *Nur77* has been reported highly expressed in the immediate/early response to feeding (44). To see whether the feeding response-induced *Nur77* expression also affects *Pparγ2* expression, we submitted fasted mice to refeeding for 2 and 8 h. As expected, the *Nur77* expression was significantly elevated after the first 2 h of refeeding compared with 8 h refeeding, remaining at a similar level as before refeeding (equal to fasted wild-type fed chow in Fig. 2C). However, there was no significant difference in *Pparγ2* expression levels at 2 and 8 h (Fig. 2D) or between $Nur77^{-/-}$ and wild-type mice under these conditions (Fig. 2D).

In summary, we observed that the fasting-induced decrease in *Pparγ2* expression is *Nur77* dependent. The analyses of the *Nur77-Pparγ* relationship in other metabolic conditions suggest that *Nur77*-dependent *Pparγ* repression is conditional and probably specific for a few conditions including a normal healthy fasting response.

Protein expression analysis of isoprenaline-treated 3T3-L1 adipocytes reflected the reverse relationship between *PPARγ* and *Nur77* expression observed at the transcriptional level. The 3T3-L1 cells expressing either a *Nur77* silencing short-hairpin construct or a nontargeting control short-hairpin were analyzed by Western blotting revealing a modest decrease in *PPARγ* expression in the control cells but not in the *Nur77*-silenced cells (Fig. 2E). Furthermore, the Nur77 protein appeared strongly elevated for several hours past the peak in transcript expression, which makes the effect on *PPARγ* expression at 4 h after induction more plausible. Protein analysis of fasted and fed wild-type and *Nur77*-knockout mice was in correspondence with the observed effects at the transcript level, showing little or no decrease in the PPARγ2 protein level in the fasted knockout mice (Fig. 2F, upper bands in the blot images). Curiously, at the protein level, the expression of the Pparγ1 protein (lower band in the blot images) also appeared differentially expressed between the wild-type and knockout mice in response to fasting. We therefore performed *Pparγ1* and *Pparγ2* isoform-specific mRNA analysis on the cohort of mice applied for the protein analysis, isolating total RNA from the remainder of the fat pads used for the protein analysis. Although a relatively minor effect is observed on *Pparγ1* expression compared with *Pparγ2*, when including a larger number of mice ($n \geq 10$), this effect proved significant within a 95% confidence interval.

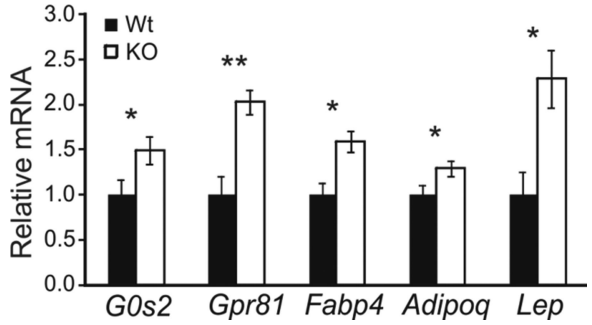

FIG. 4. *Nur77*-dependent changes in the expression of *Pparγ2* target genes. A, WAT was harvested from 24-h fasted *Nur77*$^{-/-}$ and wild-type mice. Expression of *G0s2*, *GPR81*, *Ap2*, *Adipoq*, and *Lep* was assayed with qPCR (n = 7). *, $P < 0.05$; ***, $P < 0.01$.

Because Nur77 has been known to exert functions at the cytoplasmic as well as nuclear location, we investigated the Nur77 location in the 3T3-L1 cell cultures after isoprenaline induction. For this purpose, the cells were fixed on coverslips and stained with DAPI for nuclear identification and with fluorescent immunolabeling directed against Nur77. As seen in Fig. 3, Nur77 was clearly found in the nuclei upon isoprenaline induction, confirming the possibility of a nuclear function in terms of transcriptional regulation.

Nur77-dependent effect on expression of *Pparγ2* target genes

To investigate whether the impaired decrease of *Pparγ2* expression in fasted *Nur77*$^{-/-}$ mice has extended downstream functional consequences, we studied the expression levels of known *Pparγ2* target genes. We selected several known *Pparγ2* targets from the list of differentially regulated genes in WAT from fasted *Nur77*$^{-/-}$ mice and evaluated their expression profiles with qPCR using WAT samples of a larger cohort of fasted mice (n ≥ 7). All of the assayed *Pparγ2* target genes (*G0s2*, *Gpr81*, *Fabp4*, *Adipoq*, and *Lep*) showed significantly increased mRNA levels in WAT of *Nur77*$^{-/-}$ compared with wild-type animals (Fig. 4). The Fabp4 protein level was additionally assayed by Western blotting (Fig. 2F). However, at the Western blot, only a marginal *Fabp4* expression difference was detected between fasted and fed wild-type mice. No difference was ever discernable in the fasted and fed knockout mice.

Nur77 is recruited to the *Pparγ2* promoter and represses its promoter activity

Having observed a functional connection between *Nur77* and *Pparγ2* expression in WAT during fasting, we next investigated whether the repression of *Pparγ2* expression could be assigned to a direct primary effect of the transcriptional regulatory function of *Nur77*.

In silico analysis of the mouse *Pparγ2* promoter sequence (−4000/+500 bp relative to the TSS), using a position weight matrix for Nur77 binding (NBRE), revealed several potential Nur77 binding sites at position 600, 906, 1688, 2181, and 3490 bp upstream of the TSS (Fig. 5, A, B, and D). Cross-species conservation analysis (ENSEMBL, GERP score) highlighted a highly conserved region in the proximal part of the promoter, comprising two of the predicted NBREs. Direct promoter sequence alignment showed that particularly the NBRE sequences at −600 and −906 bp were highly conserved across species and fully conserved in human (for the full sequence alignment, please see Supplemental Fig. 3). To examine whether Nur77 is recruited to the *Pparγ2* promoter, chromatin immunoprecipitation with qPCR readout (ChIP-qPCR) was performed with 3T3-L1 cells stably overexpressing *Nur77* and an antibody against Nur77. The immunoprecipitated chromatin was clearly enriched for the predicted NBRE at −600 bp and to a lesser extent for the NBRE at −906 bp compared with a non-NBRE sequence of the distal serpine 1 (*Pai-1*) promoter (Fig. 5C). A known NBRE in the proximal serpine 1 promoter (59) was used as positive control. No Nur77 binding was detected at the other predicted NBRE sequences. In short, the ChIP-qPCR analysis showed that Nur77 was recruited to the proximal part of the *Pparγ2* promoter.

To assess whether the Nur77 recruitment affects the *Pparγ2* promoter activity, luciferase reporter gene assays were performed. *Pparγ2* promoter fragments were cloned into luciferase expression vectors (Fig. 6A) and transfected into NIH-3T3 fibroblasts together with increasing amounts of a *Nur77* expression vector. Inclusion of a −1078/+62-bp fragment of the *Pparγ2* promoter (A-luc in Fig. 6) led to more than 2-fold increased activity of the luciferase reporter construct. Titration with *Nur77* in the presence of the reporter construct repressed the *Pparγ2* promoter-dependent increase to approximately half of the intensity above the basic promoter background (Fig. 6B, *left*). When the promoter fragment was truncated at the 3′-end to include only the −900-bp NBRE (B-luc), no signal increase above the basic vector activity was observed. Titration with *Nur77* did not affect this *Pparγ2* promoter-independent basic vector activity (Fig. 6B, *middle*). When applying a longer promoter fragment including four predicted NBREs, a nearly 5-fold activity increase above basic vector activity was measured. On this higher activity background, titration with *Nur77* led to a relatively diminished repression (Fig. 6B, *right*). The shorter fragment (A-luc), showing the more pronounced *Nur77* response, was chosen for further analysis. This fragment additionally contains known *Cebpa* response elements (67). Cotransfection with a *Cebpa* expression

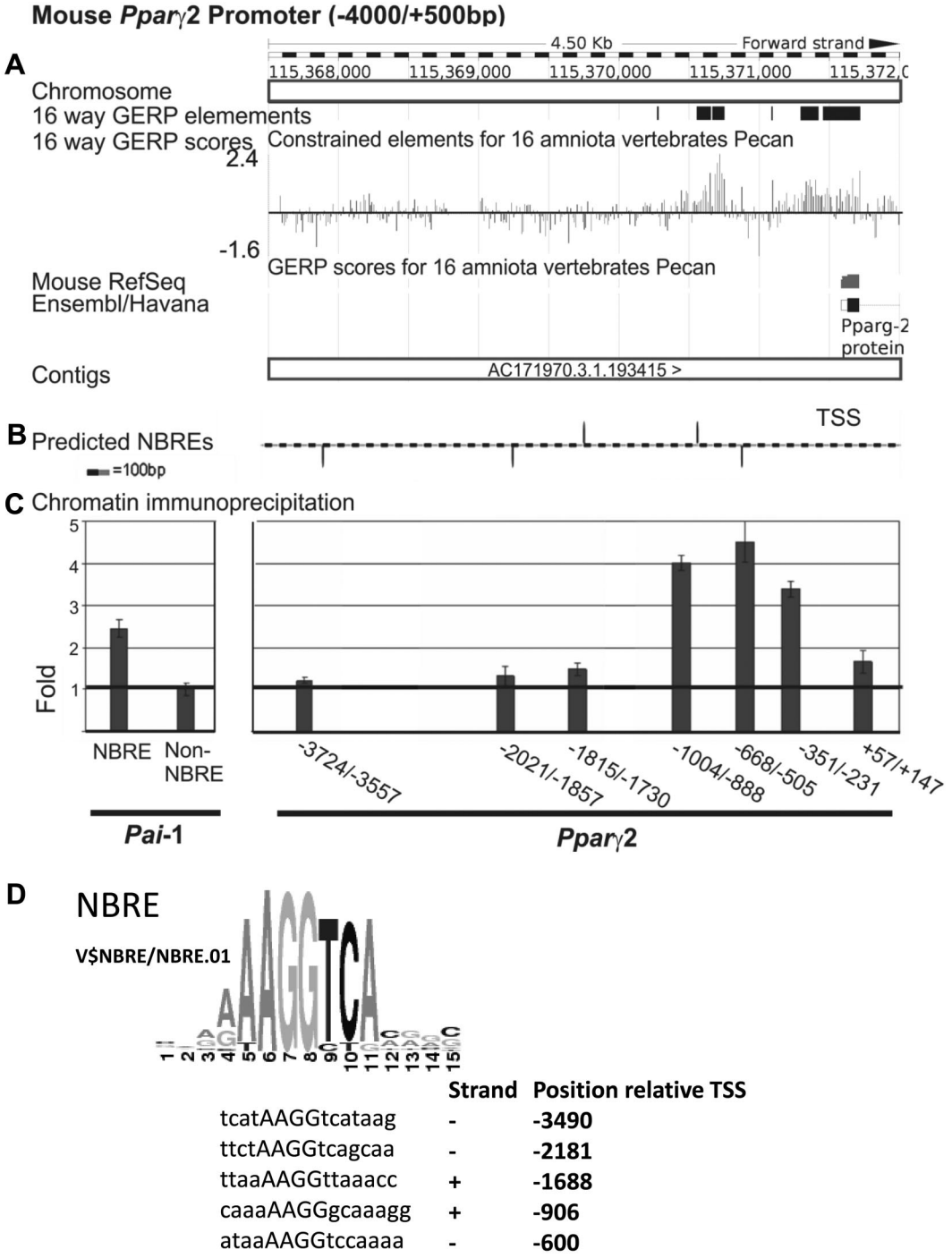

	Strand	Position relative TSS
tcatAAGGtcataag	-	-3490
ttctAAGGtcagcaa	-	-2181
ttaaAAGGttaaacc	+	-1688
caaaAAGGgcaaagg	+	-906
ataaAAGGtccaaaa	-	-600

FIG. 5. Nur77 binds to a highly conserved region of the *Pparγ2* promoter, containing predicted Nur77 binding sites (NBREs). The mouse *Pparγ2* promoter sequence, encompassing −4000/+500 bp relative to the TSS, was extracted from the CSHL promoter database. A, Cross-species conservation analysis (ENSEMBL, GERP score), showing a highly conserved region in the proximal part of the promoter. B, MatInspector analysis (Genomatix), performing a NBRE position weight matrix scan of the *Pparg2* promoter resulting in five predicted NBREs located at position −600, −906, −1688, −2181, and −3490 bp relative to the TSS, respectively. C, ChIP-qPCR of Nur77-bound chromatin from 3T3-L1 cells with constitutive Nur77 expression. Enrichment was evaluated for various amplicons within the *Pparγ2* promoter (the *bars* are aligned with the corresponding part of the promoter, shown above in B). The qPCR results were normalized to a non-NBRE-containing part of the *S18* gene (for load normalization). Enrichment is shown relative to a negative control (non-NBRE) of the *Pai-1* promoter. A previously experimentally confirmed a Nur77 binding site of the *Pai-1* promoter (NBRE) was added as positive control. The figure represents triplicate analysis of three independent experiments. D, Schematic presentation of the Nur77 NBRE position weight matrix (Genomatix V$NBRE/NBRE.01) applied for the predictions in B. Below, the sequences of the predicted NBREs are shown.

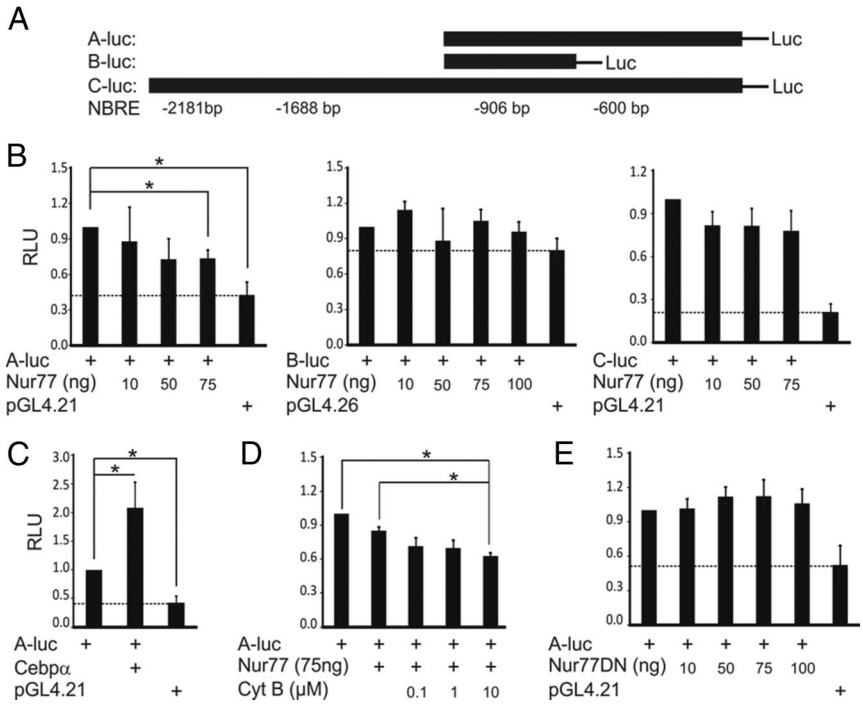

FIG. 6. *Nur77* represses the *Pparγ2* promoter activity. A, fragments of the *Pparγ2* promoter were cloned into luciferase reporter vectors and used for luciferase assays in NIH-3T3 cells. Predicted NBREs are indicated relative to the TSS. B, luciferase assays were carried out after transfection with increasing amounts of a *Nur77* expression vector and luciferase reporter vectors containing different fragments of the *Pparγ2* promoter (A-luc, B-luc, and C-luc). B, Cotransfection of a *Cebpα* expression vector with the A-luc luciferase reporter vector. D, Luciferase assay of cells transfected with the reporter vector, A-luc, and 75 ng of a *Nur77* expression vector. After transfection, increasing amounts of the Nur77 ligand cytosporone B (Cyt B) were added as indicated. E, Luciferase assays of cells transfected with the reporter vector, A-luc, and increasing amounts of a *Nur77DN* expression vector. For all assays, a renilla expression vector was employed as a transfection efficiency control. *Stippled lines* indicate the base activity of the luciferase reporter vector without promoter inserts. RLU, Relative light units. *, $P < 0.05$; $n \geq 3$.

vector further enhanced the promoter activity, confirming the integrity of the construct (Fig. 6C). Cotransfecting the *Nur77* expression vector did not significantly affect the *Cebpa*-dependent activity (data not shown).

Adding the Nur77 ligand, cytosporone B, slightly, but significantly, further enhanced the *Nur77*-dependent repression of the *Pparγ2* promoter construct (Fig. 6D). Finally, because the transcriptional regulatory function of Nur77 has predominantly been assigned to the Nur77 N-terminal domain, known to be responsible for cofactor recruitment (68, 69), we exchanged the *Nur77* expression vector for a vector expressing N-terminally truncated *Nur77* (*Nur77DN*). Contrary to the full-length receptor, titration of the *Nur77DN* construct against the −1078/+62-bp promoter fragment-containing vector did not repress the promoter activity. In summary, it appeared that Nur77 is capable of binding and repressing the proximal *Pparγ2* promoter in a ligand-enhanced manner and dependent on the N-terminal transcriptional regulatory function of Nur77.

Next, we performed *in silico* promoter analysis for NBRE of the rest of the differentially expressed genes, revealed by the microarray expression analysis. We extracted the proximal promoter sequences (−2000 bp upstream of first known RefSeq TSS and extending 500 bp downstream from last known RefSeq TSS) and applied analysis settings identical to those applied for the *Pparγ2* promoter. With this approach, 83 of the 135 promoters were positive for putative NBREs (Supplemental Table 1). This included more than half of the network-associated genes. Finally, because we had identified a significant effect on the hub component, *Pparγ2*, we compared the list of differentially expressed genes against experimentally verified ChIP-seq data from mature adipocytes (57, 58) and found the majority of the network-associated, differentially expressed genes to be within the group of validated *Pparγ2* targets (Supplemental Table 1). This argues for Nur77-dependent *Pparg2* regulation being a primary driver for changes in the gene expression in WAT of $Nur77^{-/-}$ *vs.* wild-type mice. Because several of the genes had both PPREs and putative NBREs, it is possible that the Nur77 effect on expression of *PPARγ* target genes may be both direct as well as indirect through *PPARγ* regulation.

Discussion

Pparγ2 is a well-characterized central component in adipogenesis and adipose tissue metabolism. Nevertheless, regulation at the *Pparγ2* promoter beyond terminal adipogenesis is still a fairly uncharted area. Recently, regulated *Nur77* expression in adipocytes has been identified under varying metabolic conditions. Nur77 is known to block adipogenesis within the early phase, precluding the expression of *Pparγ2* (44–46). In mature adipocytes, *Nur77* mediates insulin-stimulated glucose uptake (70). Recently, it was shown that *Nur77* expression is induced in WAT in response to conditions of β-adrenergic stimulation and fasting (27–30, 71). Yet, the underlying mechanisms, through which Nur77 may exert its effect on adipocytes, remained open for further investigation.

In this study, we performed transcriptome analysis of *Nur77*-dependent gene expression in epididymal WAT from fasted mice and found fasting-mediated repression of *Pparγ2* expression to be directly regulated by *Nur77* expression. Microarray analysis revealed a core of 135 genes differentially expressed between fasted *Nur77*$^{-/-}$ mice and their wild-type siblings. Network analysis of these genes using curated connectivity information (IPA) revealed that among the deregulated genes, *Pparγ2*, *Nur77*, and β-catenin (β1 isoform, *Ctnnb1*) form central hubs in the network. Both *Nur77* and *Ctnnb1* are known as anti-adipogenic factors in early and *Tnfα*-affected adipogenesis (49, 72–74). The observed increased expression of *Pparγ2* and decreased expression of *Ctnnb1* in the fasted *Nur77*$^{-/-}$ mice are therefore in accordance with their proposed opposite roles in adipogenesis.

Computational analysis of the *Ctnnb1* and *Pparγ2* promoters revealed highly conserved NBREs in the proximal *Pparγ2* promoter, whereas no obvious NBREs could be identified within the *Ctnnb1* promoter. ChIP-qPCR and luciferase reporter assays distinctly revealed the −1078/+62-bp (relative TSS) proximal promoter region of the *Pparγ2* promoter to be bound and repressed by *Nur77*. The repressive effect of *Nur77* on the *Pparγ2* promoter activity can be mediated through several mechanisms. The proximal part of the *Pparγ2* promoter is generally highly conserved, implicating an essential sequence-dependent function and a hot spot for transcription binding sites.

Competitive DNA binding could occur because one of the NBREs is intriguingly identical to the 5′-half of a PPRE DR-1 element (Ppar response element, direct repeat with 1-bp spacing) in close proximity to the well-documented Cebp (Caat enhancer-binding protein) binding site of the *Pparγ2* promoter (67). Through competitive binding, the Pparγ autoregulatory induction would presumably be impaired by Nur77. This region has previously also been reported to be targeted by the repressive hypoxia-induced factor Dec1 (deleted in esophageal cancer 1)/Stra13 (stimulated by retinois acid 13). Although the repression was deemed indirect because no direct promoter association could be found (75), it cannot be ruled out that *Nur77* can interact with such factors. *Nur77* is further known to repress transcription when physically interacting with the glucocorticoid receptor (76).

Another mechanism could involve the interaction with the basal transcriptional machinery through cofactors. Interestingly the corepressor SMRT [silencing mediator for retinoid or thyroid-hormone receptors (nuclear receptor co-repressor 2, Ncor2)] was shown capable of directly interacting with *Nur77* in a *Nur77* N-terminal domain-dependent manner (68). In this study, we show that N-terminally truncated *Nur77* (*Nur77DN*), unlike full-length *Nur77*, does not repress transcription from the *Pparγ2* promoter. The requirement for the N-terminal domain, which also holds the major transcriptional activation domain of *Nur77*, for transcriptional repression, is consistent with observations of *Nur77* being capable of repressing adipogenesis, whereas the N-terminally truncated *Nur77DN* is not (46) (our unpublished observations). Expressing only the N-terminal domain of *Nur77* also does not block adipogenesis in 3T3-L1 cells, suggesting that direct binding of intact *Nur77* to promoters may be required for this effect (our unpublished observations).

Elevated expression of several known *Pparγ2* target genes in WAT functionally reflect the diminished fasting-mediated down-regulation of *Pparγ2* in the fasted *Nur77*$^{-/-}$ mice. The qPCR-based validation of expression levels of *Pparγ2* targets known as *bona fide* downstream mediators of *Pparγ2* function included the adipocyte fatty acid transporter *Fabp4* and the adipokines adiponectin (*Adipoq*) and leptin (*Lep*). Increased levels of Fabp4 and of Lep have been associated with obesity and the development of metabolic syndrome (77, 78), whereas *Nur77* expression has been found inversely correlated with body mass index (70, 71). Increased expression of the *Fabp4* and *Lep* fit well with the observation that *Nur77*$^{-/-}$ mice are disposed to hepatic steatosis, insulin resistance, and obesity when raised on a HFD (32). *Adipoq*, however, is down-regulated in obesity (79). Two rather novel effectors of *Pparγ2* function in WAT were additionally included in the qPCR analysis of known *Pparγ2* target genes The G0/G1 switch gene 2 (*G0s2*) encodes a negative regulator of the adipose triglyceride lipase (*Pnpla2*), performing the first step in triglyceride breakdown (80). The lactate-activated G protein-coupled receptor (*Gpr81*) functions in an autocrine and paracrine loop to mediate insulin-induced antilipolytic effects through G(i)-dependent inhibition of adenylyl cyclase (81, 82).

In accordance with the obese phenotype of *Nur77*$^{-/-}$ mice raised on HFD (32), diminished *Nur77* expression has been reported in mouse models of obesity and insulin resistance (27). Likewise, we found a significantly blunted *Nur77* expression in WAT of fasted mice, which had been kept on HFD for 6 wk before fasting. WAT from obese mice is known to exhibit a reduced β-adrenergic response (83), which may explain the diminished *Nur77* expression in ob/ob mice. However, upon 6 wk of HFD, our mice exhibited no discernible significant weight gain. It is thus tempting to speculate that the reduced *Nur77* expression may be an early effect of a HFD, precluding the obese phenotype, and maybe possibly contributing to the

development of the obese phenotype after prolonged exposure to HFD.

Although in some scenarios *Nur77* and *Pparγ2* have supporting functions (for example, both *Pparγ2* and *Nur77* enhance insulin-stimulated glucose uptake in adipocytes) (43, 70), the emerging view is that they hold opposite roles. Whereas *Nur77* inhibits adipogenesis and stimulates gluconeogenesis (30, 36), *Pparγ2* enhances adipogenesis and decreases gluconeogenesis (84–86). The reverse expression profiles of the two NRs, as evident from several studies, including this one, suggest that the repressive function of *Nur77* discovered in WAT may also occur in other organs. As observed in BAT where the expression of *Nur77* is induced by β-adrenergic stimulation (26, 27) and the expression of *Pparγ2* is repressed (87), the pattern of opposite (mutually exclusive) expression of *Nur77* and *Pparγ2* is also seen in muscle, liver, and brain during dietary restriction (88). In mouse WAT, the circadian expression patterns of the two receptors show a peak in *Nur77* expression at 4 h in the light cycle and down-regulation afterward, followed by a rise in *Pparγ2* mRNA level peaking at 4 h into the dark cycle (89).

In conclusion, the presented study places fasting-induced *Nur77* expression in WAT as a direct repressor of *Pparγ2* expression, affecting metabolically significant *Pparγ2* target genes, as well as many other genes. This strengthens the emerging role of *Nur77* as a candidate for treatment of diseases connected with aberrant metabolic regulation.

Acknowledgments

We are grateful to Martin Klingenspor (Munich Technical University, Munich, Germany) for providing us with *Nur77*$^{-/-}$ founder mice.

Address all correspondence and requests for reprints to: A.-M. Krogsdam, Division of Bioinformatics, Biocenter, Innsbruck Medical University, 6020 Innsbruck, Austria. E-mail: anne.krogsdam@i-med.ac.at.

This work was supported by Austrian Research Council SFB Project F30, "Lipotoxicity: Lipid-Induced Cell Dysfunction and Cell Death," SFB Project 021, "Cell Proliferation and Cell Death in Tumors," and the Austrian Ministry for Science and Research; GEN-AU Projects GOLD-Genomics of Lipid-Associated Disorders; and the Bioinformatics Integration Network.

Disclosure Summary: K.D. and A.-M.K. were supported by the Austrian Research Council grant: F30, AP was supported by the Austrian Research Council grant: GOLD: FFG 820979 C3. KD's current address: Center for Integrative Genomics, Lausanne University, Lausanne, Schwitzerland.

References

1. **Heald M, Cawthorne MA** 2011 Dual acting and pan-PPAR activators as potential anti-diabetic therapies. Handb Exp Pharmacol 203:35–51
2. **Higgins LS, Depaoli AM** 2010 Selective peroxisome proliferator-activated receptor γ (PPARγ) modulation as a strategy for safer therapeutic PPARγ activation. Am J Clin Nutr 91:267S–272S
3. **Doshi LS, Brahma MK, Bahirat UA, Dixit AV, Nemmani KV** 2010 Discovery and development of selective PPARγ modulators as safe and effective antidiabetic agents. Expert Opin Investig Drugs 19: 489–512
4. **Tontonoz P, Spiegelman BM** 2008 Fat and beyond: the diverse biology of PPARγ. Annu Rev Biochem 77:289–312
5. **Zhu Y, Qi C, Korenberg JR, Chen XN, Noya D, Rao MS, Reddy JK** 1995 Structural organization of mouse peroxisome proliferator-activated receptor γ (mPPAR γ) gene: alternative promoter use and different splicing yield two mPPAR γ isoforms. Proc Natl Acad Sci USA 92:7921–7925
6. **Chen Y, Jimenez AR, Medh JD** 2006 Identification and regulation of novel PPAR-[γ] splice variants in human THP-1 macrophages. Biochim Biophys Acta 1759:32–43
7. **Sugii S, Olson P, Sears DD, Saberi M, Atkins AR, Barish GD, Hong SH, Castro GL, Yin YQ, Nelson MC, Hsiao G, Greaves DR, Downes M, Yu RT, Olefsky JM, Evans RM** 2009 PPARγ activation in adipocytes is sufficient for systemic insulin sensitization. Proc Natl Acad Sci USA 106:22504–22509
8. **Evans RM, Barish GD, Wang YX** 2004 PPARs and the complex journey to obesity. Nat Med 10:355–361
9. **Rosen ED, Spiegelman BM** 2001 PPARγ : a nuclear regulator of metabolism, differentiation, and cell growth. J Biol Chem 276: 37731–37734
10. **White UA, Stephens JM** 2010 Transcriptional factors that promote formation of white adipose tissue. Mol Cell Endocrinol 318:10–14
11. **Kintscher U, Law RE** 2005 PPARγ-mediated insulin sensitization: the importance of fat versus muscle. Am J Physiol Endocrinol Metab 288:E287–E291
12. **Gray SL, Nora ED, Grosse J, Manieri M, Stoeger T, Medina-Gomez G, Burling K, Wattler S, Russ A, Yeo GS, Chatterjee VK, O'Rahilly S, Voshol PJ, Cinti S, Vidal-Puig A** 2006 Leptin deficiency unmasks the deleterious effects of impaired peroxisome proliferator-activated receptor γ function (P465L PPARγ) in mice. Diabetes 55: 2669–2677
13. **He W, Barak Y, Hevener A, Olson P, Liao D, Le J, Nelson M, Ong E, Olefsky JM, Evans RM** 2003 Adipose-specific peroxisome proliferator-activated receptor γ knockout causes insulin resistance in fat and liver but not in muscle. Proc Natl Acad Sci USA 100:15712–15717
14. **Villacorta L, Schopfer FJ, Zhang J, Freeman BA, Chen YE** 2009 PPARγ and its ligands: therapeutic implications in cardiovascular disease. Clin Sci (Lond) 116:205–218
15. **Forman BM, Chen J, Evans RM** 1996 The peroxisome proliferator-activated receptors: ligands and activators. Ann NY Acad Sci 804: 266–275
16. **Willson TM, Lehmann JM, Kliewer SA** 1996 Discovery of ligands for the nuclear peroxisome proliferator-activated receptors. Ann NY Acad Sci 804:276–283
17. **Lenhard JM** 2001 PPAR γ/RXR as a molecular target for diabetes. Receptors Channels 7:249–258
18. **Bogner-Strauss JG, Prokesch A, Sanchez-Cabo F, Rieder D, Hackl H, Duszka K, Krogsdam A, Di Camillo B, Walenta E, Klatzer A, Lass A, Pinent M, Wong WC, Eisenhaber F, Trajanoski Z** 2010 Reconstruction of gene association network reveals a transmembrane protein required for adipogenesis and targeted by PPARγ. Cell Mol Life Sci 67:4049–4064
19. **Prokesch A, Bogner-Strauss JG, Hackl H, Rieder D, Neuhold C, Walenta E, Krogsdam A, Scheideler M, Papak C, Wong WC, Vin-**

son C, Eisenhaber F, Trajanoski Z 2011 Arxes: retrotransposed genes required for adipogenesis. Nucleic Acids Res 39:3224–3239
20. **Smith AG, Luk N, Newton RA, Roberts DW, Sturm RA, Muscat GE** 2008 Melanocortin-1 receptor signaling markedly induces the expression of the NR4A nuclear receptor subgroup in melanocytic cells. J Biol Chem 283:12564–12570
21. **Wang SC, Myers SA, Eriksson NA, Fitzsimmons RL, Muscat GE** 2011 *Nr4a1* siRNA expression attenuates α-MSH regulated gene expression in 3T3-L1 adipocytes. Mol Endocrinol 25:291–306
22. **McMorrow JP, Murphy EP** 2011 Inflammation: a role for NR4A orphan nuclear receptors? Biochem Soc Trans 39:688–693
23. **Zhao Y, Howatt DA, Gizard F, Nomiyama T, Findeisen HM, Heywood EB, Jones KL, Conneely OM, Daugherty A, Bruemmer D** 2010 Deficiency of the NR4A orphan nuclear receptor NOR1 decreases monocyte adhesion and atherosclerosis. Circ Res 107:501–511
24. **Pearen MA, Muscat GE** 2010 Nuclear hormone receptor 4A signaling: implications for metabolic disease. Mol Endocrinol 24:1891–1903
25. **Maxwell MA, Muscat GE** 2006 The NR4A subgroup: immediate early response genes with pleiotropic physiological roles. Nucl Recept Signal 4:e002
26. **Kanzleiter T, Schneider T, Walter I, Bolze F, Eickhorst C, Heldmaier G, Klaus S, Klingenspor M** 2005 Evidence for Nr4a1 as a cold-induced effector of brown fat thermogenesis. Physiol Genomics 24:37–44
27. **Kumar N, Liu D, Wang H, Robidoux J, Collins S** 2008 Orphan nuclear receptor NOR-1 enhances 3′,5′-cyclic adenosine 5′-monophosphate-dependent uncoupling protein-1 gene transcription. Mol Endocrinol 22:1057–1064
28. **Maxwell MA, Cleasby ME, Harding A, Stark A, Cooney GJ, Muscat GE** 2005 Nur77 regulates lipolysis in skeletal muscle cells. Evidence for cross-talk between the β-adrenergic and an orphan nuclear hormone receptor pathway. J Biol Chem 280:12573–12584
29. **Myers SA, Eriksson N, Burow R, Wang SC, Muscat GE** 2009 β-Adrenergic signaling regulates NR4A nuclear receptor and metabolic gene expression in multiple tissues. Mol Cell Endocrinol 309:101–108
30. **Pei L, Waki H, Vaitheesvaran B, Wilpitz DC, Kurland IJ, Tontonoz P** 2006 NR4A orphan nuclear receptors are transcriptional regulators of hepatic glucose metabolism. Nat Med 12:1048–1055
31. **Bachman ES, Dhillon H, Zhang CY, Cinti S, Bianco AC, Kobilka BK, Lowell BB** 2002 βAR signaling required for diet-induced thermogenesis and obesity resistance. Science 297:843–845
32. **Chao LC, Wroblewski K, Zhang Z, Pei L, Vergnes L, Ilkayeva OR, Ding SY, Reue K, Watt MJ, Newgard CB, Pilch PF, Hevener AL, Tontonoz P** 2009 Insulin resistance and altered systemic glucose metabolism in mice lacking Nur77. Diabetes 58:2788–2796
33. **Fortier M, Wang SP, Mauriège P, Semache M, Mfuma L, Li H, Levy E, Richard D, Mitchell GA** 2004 Hormone-sensitive lipase-independent adipocyte lipolysis during β-adrenergic stimulation, fasting, and dietary fat loading. Am J Physiol Endocrinol Metab 287:E282–E288
34. **McConville P, Fishbein KW, Lakatta EG, Spencer RG** 2003 Differences in the bioenergetic response of the isolated perfused rat heart to selective β1- and β2-adrenergic receptor stimulation. Circulation 107:2146–2152
35. **McConville P, Lakatta EG, Spencer RG** 2007 Greater glycogen utilization during 1- than 2-adrenergic receptor stimulation in the isolated perfused rat heart. Am J Physiol Endocrinol Metab 293:E1828–E1835
36. **Pols TW, Ottenhoff R, Vos M, Levels JH, Quax PH, Meijers JC, Pannekoek H, Groen AK, de Vries CJ** 2008 Nur77 modulates hepatic lipid metabolism through suppression of SREBP1c activity. Biochem Biophys Res Commun 366:910–916
37. **Robidoux J, Kumar N, Daniel KW, Moukdar F, Cyr M, Medvedev AV, Collins S** 2006 Maximal β3-adrenergic regulation of lipolysis involves Src and epidermal growth factor receptor-dependent ERK1/2 activation. J Biol Chem 281:37794–37802
38. **Yamamoto DL, Hutchinson DS, Bengtsson T** 2007 β_2-Adrenergic activation increases glycogen synthesis in L6 skeletal muscle cells through a signalling pathway independent of cyclic AMP. Diabetologia 50:158–167
39. **Kagaya S, Ohkura N, Tsukada T, Miyagawa M, Sugita Y, Tsujimoto G, Matsumoto K, Saito H, Hashida R** 2005 Prostaglandin A2 acts as a transactivator for NOR1 (NR4A3) within the nuclear receptor superfamily. Biol Pharm Bull 28:1603–1607
40. **Wansa KD, Harris JM, Yan G, Ordentlich P, Muscat GE** 2003 The AF-1 domain of the orphan nuclear receptor NOR-1 mediates trans-activation, coactivator recruitment, and activation by the purine anti-metabolite 6-mercaptopurine. J Biol Chem 278:24776–24790
41. **Yoo YG, Na TY, Yang WK, Kim HJ, Lee IK, Kong G, Chung JH, Lee MO** 2007 6-Mercaptopurine, an activator of Nur77, enhances transcriptional activity of HIF-1α resulting in new vessel formation. Oncogene 26:3823–3834
42. **Lee SO, Li X, Khan S, Safe S** 2011 Targeting NR4A1 (TR3) in cancer cells and tumors. Expert Opin Ther Targets 15:195–206
43. **Zhan Y, Du X, Chen H, Liu J, Zhao B, Huang D, Li G, Xu Q, Zhang M, Weimer BC, Chen D, Cheng Z, Zhang L, Li Q, Li S, Zheng Z, Song S, Huang Y, Ye Z, Su W, Lin SC, Shen Y, Wu Q** 2008 Cytosporone B is an agonist for nuclear orphan receptor Nur77. Nat Chem Biol 4:548–556
44. **Chao LC, Bensinger SJ, Villanueva CJ, Wroblewski K, Tontonoz P** 2008 Inhibition of adipocyte differentiation by Nur77, Nurr1, and Nor1. Mol Endocrinol 22:2596–2608
45. **Fumoto T, Yamaguchi T, Hirose F, Osumi T** 2007 Orphan nuclear receptor Nur77 accelerates the initial phase of adipocyte differentiation in 3T3-L1 cells by promoting mitotic clonal expansion. J Biochem 141:181–192
46. **Au WS, Payne VA, O'Rahilly S, Rochford JJ** 2008 The NR4A family of orphan nuclear receptors are not required for adipogenesis. Int J Obes (Lond) 32:388–392
47. **Lee SL, Wesselschmidt RL, Linette GP, Kanagawa O, Russell JH, Milbrandt J** 1995 Unimpaired thymic and peripheral T cell death in mice lacking the nuclear receptor NGFI-B (Nur77). Science 269:532–535
48. **Yamamoto Y, Gesta S, Lee KY, Tran TT, Saadatirad P, Kahn CR** 2010 Adipose depots possess unique developmental gene signatures. Obesity 18:872–878
49. **Suzuki S, Suzuki N, Mirtsos C, Horacek T, Lye E, Noh SK, Ho A, Bouchard D, Mak TW, Yeh WC** 2003 Nur77 as a survival factor in tumor necrosis factor signaling. Proc Natl Acad Sci USA 100:8276–8280
50. **Zhao S, Fernald RD** 2005 Comprehensive algorithm for quantitative real-time polymerase chain reaction. J Comput Biol 12:1047–1064
51. **Pabinger S, Thallinger GG, Snajder R, Eichhorn H, Rader R, Trajanoski Z** 2009 QPCR: application for real-time PCR data management and analysis. BMC Bioinformatics 10:268
52. **Hackl H, Burkard TR, Sturn A, Rubio R, Schleiffer A, Tian S, Quackenbush J, Eisenhaber F, Trajanoski Z** 2005 Molecular processes during fat cell development revealed by gene expression profiling and functional annotation. Genome Biol 6:R108
53. **Rainer J, Sanchez-Cabo F, Stocker G, Sturn A, Trajanoski Z** 2006 CARMAweb: comprehensive R- and bioconductor-based web service for microarray data analysis. Nucleic Acids Res 34:W498–W503
54. **Gentleman RC, Carey VJ, Bates DM, Bolstad B, Dettling M, Dudoit S, Ellis B, Gautier L, Ge Y, Gentry J, Hornik K, Hothorn T, Huber W, Iacus S, Irizarry R, Leisch F, Li C, Maechler M, Rossini AJ, Sawitzki G, Smith C, Smyth G, Tierney L, Yang JY, Zhang J** 2004 Bioconductor: open software development for computational biology and bioinformatics. Genome Biol 5:R80

55. **Hochberg Y, Benjamini Y** 1990 More powerful procedures for multiple significance testing. Stat Med 9:811–818
56. **Calvano SE, Xiao W, Richards DR, Felciano RM, Baker HV, Cho RJ, Chen RO, Brownstein BH, Cobb JP, Tschoeke SK, Miller-Graziano C, Moldawer LL, Mindrinos MN, Davis RW, Tompkins RG, Lowry SF; Inflamm and Host Response to Injury Large Scale Collab Res Program** 2005 A network-based analysis of systemic inflammation in humans. Nature 437:1032–1037
57. **Nielsen R, Pedersen TA, Hagenbeek D, Moulos P, Siersbaek R, Megens E, Denissov S, Børgesen M, Francoijs KJ, Mandrup S, Stunnenberg HG** 2008 Genome-wide profiling of PPARγ:RXR and RNA polymerase II occupancy reveals temporal activation of distinct metabolic pathways and changes in RXR dimer composition during adipogenesis. Genes Dev 22:2953–2967
58. **Lefterova MI, Zhang Y, Steger DJ, Schupp M, Schug J, Cristancho A, Feng D, Zhuo D, Stoeckert Jr CJ, Liu XS, Lazar MA** 2008 PPARγ and C/EBP factors orchestrate adipocyte biology via adjacent binding on a genome-wide scale. Genes Dev 22:2941–2952
59. **Gruber F, Hufnagl P, Hofer-Warbinek R, Schmid JA, Breuss JM, Huber-Beckmann R, Lucerna M, Papac N, Harant H, Lindley I, de Martin R, Binder BR** 2003 Direct binding of Nur77/NAK-1 to the plasminogen activator inhibitor 1 (PAI-1) promoter regulates TNFα-induced PAI-1 expression. Blood 101:3042–3048
60. **Kanzleiter T, Wilks D, Preston E, Ye J, Frangioudakis G, Cooney GJ** 2009 Regulation of the nuclear hormone receptor nur77 in muscle: influence of exercise-activated pathways in vitro and obesity in vivo. Biochim Biophys Acta 1792:777–782
61. **Javerzat JP** 2010 Directing the Centromere Guardian. Science 327: 150–151
62. **Chen D, Gould C, Garza R, Gao T, Hampton RY, Newton AC** 2007 Amplitude control of protein kinase C by RINCK, a novel E3 ubiquitin ligase. J Biol Chem 282:33776–33787
63. **Carpenter B, Hill KJ, Charalambous M, Wagner KJ, Lahiri D, James DI, Andersen JS, Schumacher V, Royer-Pokora B, Mann M, Ward A, Roberts SGE** 2004 BASP1 is a transcriptional cosuppressor for the Wilms' tumor suppressor protein WT1. Mol Cell Biol 24:537–549
64. **Christodoulides C, Lagathu C, Sethi JK, Vidal-Puig A** 2009 Adipogenesis and WNT signalling. Trends Endocrinol Metab 20:16–24
65. **Dackor R, Fritz-Six K, Smithies O, Caron K** 2007 Receptor activity-modifying proteins 2 and 3 have distinct physiological functions from embryogenesis to old age. J Biol Chem 282:18094–18099
66. **Chao LC, Zhang Z, Pei L, Saito T, Tontonoz P, Pilch PF** 2007 Nur77 coordinately regulates expression of genes linked to glucose metabolism in skeletal muscle. Mol Endocrinol 21:2152–2163
67. **Clarke SL, Robinson CE, Gimble JM** 1997 CAAT/enhancer binding proteins directly modulate transcription from the peroxisome proliferator-activated receptor γ2 promoter. Biochem Biophys Res Commun 240:99–103
68. **Sohn YC, Kwak E, Na Y, Lee JW, Lee SK** 2001 Silencing mediator of retinoid and thyroid hormone receptors and activating signal cointegrator-2 as transcriptional coregulators of the orphan nuclear receptor Nur77. J Biol Chem 276:43734–43739
69. **Park KC, Song KH, Chung HK, Kim H, Kim DW, Song JH, Hwang ES, Jung HS, Park SH, Bae I, Lee IK, Choi HS, Shong M** 2005 CR6-interacting factor 1 interacts with orphan nuclear receptor Nur77 and inhibits its transactivation. Mol Endocrinol 19:12–24
70. **Fu Y, Luo L, Luo N, Zhu X, Garvey WT** 2007 NR4A orphan nuclear receptors modulate insulin action and the glucose transport system: potential role in insulin resistance. J Biol Chem 282:31525–31533
71. **Kanzleiter T, Preston E, Wilks D, Ho B, Benrick A, Reznick J, Heilbronn LK, Turner N, Cooney GJ** 2010 Overexpression of the orphan receptor Nur77 alters glucose metabolism in rat muscle cells and rat muscle in vivo. Diabetologia 53:1174–1183
72. **Ross SE, Hemati N, Longo KA, Bennett CN, Lucas PC, Erickson RL, MacDougald OA** 2000 Inhibition of adipogenesis by Wnt signaling. Science 289:950–953
73. **Kennell JA, MacDougald OA** 2005 Wnt signaling inhibits adipogenesis through β-catenin-dependent and -independent mechanisms. J Biol Chem 280:24004–24010
74. **Gustafson B, Smith U** 2006 Cytokines promote Wnt signaling and inflammation and impair the normal differentiation and lipid accumulation in 3T3-L1 preadipocytes. J Biol Chem 281:9507–9516
75. **Yun Z, Maecker HL, Johnson RS, Giaccia AJ** 2002 Inhibition of PPAR γ2 gene expression by the HIF-1-regulated gene DEC1/Stra13: a mechanism for regulation of adipogenesis by hypoxia. Dev Cell 2:331–341
76. **Philips A, Maira M, Mullick A, Chamberland M, Lesage S, Hugo P, Drouin J** 1997 Antagonism between Nur77 and glucocorticoid receptor for control of transcription. Mol Cell Biol 17:5952–5959
77. **Karakas SE, Almario RU, Kim K** 2009 Serum fatty acid binding protein 4, free fatty acids, and metabolic risk markers. Metabolism 58:1002–1007
78. **Murer SB, Knöpfli BH, Aeberli I, Jung A, Wildhaber J, Wildhaber-Brooks J, Zimmermann MB** 2011 Baseline leptin and leptin reduction predict improvements in metabolic variables and long-term fat loss in obese children and adolescents: a prospective study of an inpatient weight-loss program. Am J Clin Nutr 93:695–702
79. **Hu E, Liang P, Spiegelman BM** 1996 AdipoQ is a novel adipose-specific gene dysregulated in obesity. J Biol Chem 271:10697–10703
80. **Yang X, Lu X, Lombès M, Rha GB, Chi YI, Guerin TM, Smart EJ, Liu J** 2010 The G_0/G_1 switch gene 2 regulates adipose lipolysis through association with adipose triglyceride lipase. Cell Metab 11:194–205
81. **Jeninga EH, Bugge A, Nielsen R, Kersten S, Hamers N, Dani C, Wabitsch M, Berger R, Stunnenberg HG, Mandrup S, Kalkhoven E** 2009 Peroxisome proliferator-activated receptor γ regulates expression of the anti-lipolytic G-protein-coupled receptor 81 (GPR81/Gpr81). J Biol Chem 284:26385–26393
82. **Ahmed K, Tunaru S, Tang C, Müller M, Gille A, Sassmann A, Hanson J, Offermanns S** 2010 An autocrine lactate loop mediates insulin-dependent inhibition of lipolysis through GPR81. Cell Metab 11:311–319
83. **Collins S, Daniel KW, Rohlfs EM, Ramkumar V, Taylor IL, Gettys TW** 1994 Impaired expression and functional activity of the β-3 and β-1 adrenergic receptor in adipose tissue of congenitally obese (C57BLJ6-ob/ob) mice. Mol Endocrinol 8:518–527
84. **Way JM, Harrington WW, Brown KK, Gottschalk WK, Sundseth SS, Mansfield TA, Ramachandran RK, Willson TM, Kliewer SA** 2001 Comprehensive messenger ribonucleic acid profiling reveals that peroxisome proliferator-activated receptor γ activation has coordinate effects on gene expression in multiple insulin-sensitive tissues. Endocrinology 142:1269–1277
85. **Schadinger SE, Bucher NL, Schreiber BM, Farmer SR** 2005 PPARγ2 regulates lipogenesis and lipid accumulation in steatotic hepatocytes. Am J Physiol Endocrinol Metab 288:E1195–E1205
86. **Zhang YL, Hernandez-Ono A, Siri P, Weisberg S, Conlon D, Graham MJ, Crooke RM, Huang LS, Ginsberg HN** 2006 Aberrant hepatic expression of PPARγ2 stimulates hepatic lipogenesis in a mouse model of obesity, insulin resistance, dyslipidemia, and hepatic steatosis. J Biol Chem 281:37603–37615
87. **Lindgren EM, Nielsen R, Petrovic N, Jacobsson A, Mandrup S, Cannon B, Nedergaard J** 2004 Noradrenaline represses PPAR (peroxisome-proliferator-activated receptor) γ2 gene expression in brown adipocytes: intracellular signalling and effects on PPARγ2 and PPARγ1 protein levels. Biochem J 382:597–606
88. **Oita RC, Mazzatti DJ, Lim FL, Powell JR, Merry BJ** 2009 Whole-genome microarray analysis identifies up-regulation of Nr4a nuclear receptors in muscle and liver from diet-restricted rats. Mech Ageing Dev 130:240–247
89. **Yang X, Downes M, Yu RT, Bookout AL, He W, Straume M, Mangelsdorf DJ, Evans RM** 2006 Nuclear receptor expression links the circadian clock to metabolism. Cell 126:801–810